FAST DUAL-BASELINE QUAD-POL RETRIEVAL OF FOREST HEIGHT AND DIGITAL TERRAIN MODEL: THE BIOMASS CASE

Roman Guliaev, Matteo Pardini, Konstantinos P. Papathanassiou

German Aerospace Center (DLR), Microwave and Radar Institute (HR), Wessling (Germany)

ABSTRACT

The future BIOMASS mission will collect groundbreaking large-scale spaceborne polarimetric, repeat-pass interferometric, and tomographic data. The main objective of the mission is to produce forest height and biomass maps. The repeat-pass configuration requires accounting for temporal decorrelation, which affects forest height and digital terrain model retrieval. The knowledge about the vertical reflectivity profile (VRP) from the tomographic stage of the mission allows for reducing the dimensionality to the 11-parameter problem (dual-baseline quad-pol case). This paper proposes to further simplify the inversion process by reformulating the problem into a simpler 2-parameter ground and forest height retrieval.

***Index Terms*—** PolInSAR, Forest height, Digital terrain model

1. INTRODUCTION

1.1. Interferometric volumetric decorrelation

Polarimetric Synthetic Aperture Radar Interferometry (PolInSAR) estimates volumetric decorrelation as a Fourier transform of the (normalized) vertical reflectivity profile $F(z,\vec{w})$ within the reflectivity volume, i.e. from the bottom to the top of the forested layer h_v, adjusted to the underlying ground height z_0

$$\tilde{\gamma}_{Vol}(k_z,\vec{w}) = e^{jk_z z_0}\frac{\int_0^{h_V} F(z,\vec{w})\,\exp(jk_z\ z)dz}{\int_0^{h_V} F(z,\vec{w})\,dz}. \qquad (1)$$

The vertical wavenumber k_z is proportional to the look angle difference $\Delta\theta$ between the two acquisitions and inverse proportional to the incidence angle θ_0

$$k_z = \frac{4\pi}{\lambda}\frac{\Delta\theta}{\sin(\theta_0)}. \qquad (2)$$

In the context of a two-layer (volume and ground) inversion model the vertical reflectivity can be modelled as

$$F(z,\vec{w}) = f_V(z) + m(\vec{w})\delta(z - z_0) \qquad (3)$$

where $m(\vec{w})$ is the ground-to-volume ratio. Following the Random Volume over Ground (RVoG) model [1] [2] the volume only reflectivity $f_V(z)$ is assumed to be polarization independent. The equation (1) can be rewritten as

$$\tilde{\gamma}_{Vol}(\kappa_z,\vec{w}) = \tilde{\gamma}_V(\kappa_z) + L(\vec{w})\big(1 - \tilde{\gamma}_V(k_z)\big). \qquad (4)$$

where $L(\vec{w}) = m(\vec{w})/(1 + m(\vec{w}))$ is the polarization dependent term and $\tilde{\gamma}_V(k_z)$ is the volume-only volumetric decorrelation

$$\tilde{\gamma}_V(\kappa_z) = e^{jk_z z_0}\frac{\int_0^1 f_V(z)\exp(jk_z h_v\ z)dz}{\int_0^1 f_V(z)\,dz}. \qquad (5)$$

According to (4) and (5), if the vertical reflectivity $F(z',\vec{w})$ is known, forest height can be inverted, by means of a balanced inversion problem, from a single $\tilde{\gamma}_{Vol}(\kappa_z,\vec{w})$ measurement.

1.2. Tomographic reconstruction of vertical reflectivity profiles

SAR Tomography (TomoSAR) estimates the profile of the backscattered vertical power profiles $P(z,\vec{w})$ as a function of the height z and polarization $\vec{w}$. It relies on a set of single-look complex (SLC) SAR images $s_1(\vec{w}), s_2(\vec{w}), \dots, s_M(\vec{w})$ acquired along spatially (and temporal) displaced tracks. The set of the M co-registered and (phase) calibrated SLC images forms the so-called tomographic (data) stack and can be written in form of a (column) data vector $\vec{y}(\vec{w}) = [s_1(\vec{w}), s_2(\vec{w}), \dots, s_M(\vec{w})]^T$ [3] with (M×M)-dimensional covariance matrix:

$$[R] := < \vec{y}(\vec{w}) \cdot \vec{y}^H(\vec{w}) > \qquad (6)$$

with $R_{mn} = < s_m(\vec{w})\, s_n^*(\vec{w}) >$. Each element R_{mn} of [R] corresponds to an image pair formed by the m-th and n-th image of the stack and can be related to the vertical reflectivity profile via a Fourier relation:

$$R_{mn} = \int F(z,\vec{w})\, e^{jk_z^{mn} z}\, dz \qquad (7)$$

where k_z^{mn} is the vertical wavenumber associated to the pair formed by the m-th and the n-th images of the stack:

$$k_z^{mn} := 2\frac{2\pi}{\lambda}\frac{\Delta\theta^{mn}}{\sin(\theta_0)} \tag{8}$$

To distinguish the different scattering mechanisms, the sum of Kronecker products (SKP) algorithm was proposed. In the simplest case of two scattering mechanisms: ground and volume, the covariance matrix can be approximated as [4]:

$$[R_p] = [C_{3G}]\otimes[\Gamma_{MG}] + [C_{3V}]\otimes[\Gamma_{MV}] \tag{9}$$

where $[\Gamma_{MG}]$ and $[\Gamma_{MV}]$ are ground and volume tomographic coherence matrices and $[C_{3G}]$ and $[C_{3V}]$ are its corresponding polarimetric covariance matrices.
The volume-only vertical power profile can be reconstructed from volume covariance matrix [5]

$$P_V(z) = \vec{h}(z)^H[\Gamma_{MV}]\vec{h}(z) \tag{10}$$

The generic filter $\vec{h}(z)$ is designed to allow only the backscatter contribution at z_i to pass, while cancelling out the contributions at the other heights. In the following, the Fourier beamforming filter will be used.
The volume-only vertical power profiles $P_V(z)$ can be substituted as a reconstruction of volume-only vertical reflectivity profile in (5):

$$\tilde{\gamma}_V(k_z \mid f_V(z), h_v) = \frac{\int_0^1 P_V(z)\exp(jk_Z h_v\, z)dz}{\int_0^1 P_V(z)\, dz} \tag{11}$$

1.3. Dual-baseline forest height estimation

Tomographic reconstruction of vertical reflectivity profiles

The dual baseline PolInSAR case allows to account for the (real-valued) temporal decorrelations $\tilde{\gamma}_T^1$ and $\tilde{\gamma}_T^2$, affecting measurements of the volumetric decorrelations at two different baselines in repeat-pass configurations [6]

$$\tilde{\gamma}_{Vol}^i(\vec{w}) = e^{jk_{z_i}z_0}[\gamma_T^i(\vec{w})\tilde{\gamma}_V^i + L(\vec{w})\left(1-\gamma_T^i(\vec{w})\tilde{\gamma}_V^i\right)],\quad i = 1,2 \tag{12}$$

Using equation (12) with the approximated vertical reflectivity profile, the forest height can be estimated from the following 11-parameter minimisation problem:

$$\begin{aligned}&\{h_v, \phi_0, m(\vec{w}), \gamma_t^{12}(\vec{w}), \gamma_t^{23}(\vec{w})\}\\ &= \underset{h_v, z_0, m(\vec{w}), \gamma_{t1}^{12}(\vec{w}), \gamma_{t2}^{13}(\vec{w})}{\arg\min} \left\| \begin{bmatrix}\gamma_{Obs}(\vec{w}, k_z^{12})\\ \gamma_{Obs}(\vec{w}, k_z^{13})\end{bmatrix} - \begin{bmatrix}\gamma_t^{12}\gamma(k_z^{12}, \{h_V, m\})\\ \gamma_t^{13}\gamma(k_z^{13}, \{h_V, m\}\end{bmatrix}\right\|\end{aligned} \tag{13}$$

The minimisation problem (13) can be simplified by multiplying left- and right-hand sides of equation (12) by $\tilde{\gamma}_V^{i\,*}$ and considering only the imaginary part from the both sides, so that the temporal decorrelation dependency is eliminated

$$\mathrm{Im}\left[e^{-jk_{z_i}z_0}\tilde{\gamma}_{Vol}^i(\vec{w})\tilde{\gamma}_V^{i\,*}\right] = L(\vec{w})\mathrm{Im}\left[\tilde{\gamma}_V^{i\,*}\right]. \tag{14}$$

Assuming that the polarization dependent parameter $L(\vec{w})$ is not changing between acquisitions, the following relation can be obtained:

$$\frac{\mathrm{Im}\left[e^{-jk_{z_1}z_0}\tilde{\gamma}_{Vol}^1(\vec{w})\tilde{\gamma}_V^{1\,*}\right]}{\mathrm{Im}\left[\tilde{\gamma}_V^{1\,*}\right]} = \frac{\mathrm{Im}\left[e^{-jk_{z_2}z_0}\tilde{\gamma}_{Vol}^2(\vec{w})\tilde{\gamma}_V^{2\,*}\right]}{\mathrm{Im}\left[\tilde{\gamma}_V^{2\,*}\right]} \tag{15}$$

which by opening the brackets rewrites to

$$L_1(\vec{w}) = L_2(\vec{w})$$

where

$$L_i(\vec{w}) := \frac{\mathrm{Re}\left[\tilde{\gamma}_V^i\right]}{\mathrm{Im}\left[\tilde{\gamma}_V^i\right]}\mathrm{Im}\left[e^{-jk_{z_i}z_0}\tilde{\gamma}_{Vol}^i\right] - \mathrm{Re}\left[e^{-jk_{z_i}z_0}\tilde{\gamma}_{Vol}^i\right] \tag{16}$$

As can be seen from equation (16), the dependency of ground-to-volume ratio and temporal decorrelation was eliminated. The parameters $L_1(\vec{w})$ and $L_2(\vec{w})$ are polarization dependent but invariant of the vertical wavenumber k_z. With the TomoSAR approximated vertical reflectivity profile, the equation (16) establishes a direct dependency of forest height on the measured volumetric decorrelations $\tilde{\gamma}_{Vol}^1$ and $\tilde{\gamma}_{Vol}^2$, if only z_0 is found.
To estimate z_0, (16) can be rewritten inn the following way:

$$x_{12}(\vec{w}, z_0) = \alpha_1 y_1(\vec{w}, z_0) - \alpha_2 y_2(\vec{w}, z_0)$$

where

$$\begin{gathered} x_{12} = \mathrm{Re}\left[\tilde{\gamma}_{Vol}^1 e^{-jk_{z_1}z_0}\right] - \mathrm{Re}\left[\tilde{\gamma}_{Vol}^2 e^{-jk_{z_2}z_0}\right]\\ y_1 = \mathrm{Im}\left[\tilde{\gamma}_{Vol}^1 e^{-jk_{z_1}z_0}\right], y_2 = \mathrm{Im}\left[\tilde{\gamma}_{Vol}^2 e^{-jk_{z_2}z_0}\right]\\ \alpha_1 = \frac{\mathrm{Re}[\tilde{\gamma}_V^1]}{\mathrm{Im}[\tilde{\gamma}_V^1]}, \alpha_2 = \frac{\mathrm{Re}[\tilde{\gamma}_V^2]}{\mathrm{Im}[\tilde{\gamma}_V^2]}\end{gathered} \tag{17}$$

Note that coefficients α_1 and α_2 are related to volume only coherence and do not depend on polarization. Parameters x_{12}, y_1 and y_2 are measured from the observed volumetric decorrelation and are parameterised only by z_0. The following can be written for each polarization channel in the quad pol configuration, $\vec{w} = [w_1, w_2, w_3]$:

$$\begin{aligned} x_{12}(w_1, z_o) &= \alpha_1 y_1(w_1, z_o) - \alpha_2 y_2(w_1, z_o)\\ x_{12}(w_2, z_o) &= \alpha_1 y_1(w_2, z_o) - \alpha_2 y_2(w_2, z_o)\\ x_{12}(w_3, z_o) &= \alpha_1 y_1(w_3, z_o) - \alpha_2 y_2(w_3, z_o)\end{aligned} \tag{18}$$

Eliminating α_1 dependency from (18) and redefining for simplicity $x_{12}^i := x_{12}(w_i, z_o)$, $y_1^i := y_1(w_i, z_o)$, $y_2^i := y_2(w_i, z_o)$, it follows:

$$x_{12}^1 y_1^2 - x_{12}^2 y_1^1 = \alpha_2[y_2^1 y_1^2 - y_2^2 y_1^1]$$
$$x_{12}^2 y_1^3 - x_{12}^3 y_1^2 = \alpha_2[y_2^2 y_1^3 - y_2^3 y_1^2] \quad (19)$$

And finally solving the α_2, the following tensor invariant is obtained:

$$S_{12}^{12}(z_o) = S_{12}^{23}(z_o)$$

$$S_{lk}^{ij}(z_o) = \frac{x_{lk}^i y_l^j - x_{lk}^j y_l^i}{y_k^i y_l^j - y_k^j y_l^i} \quad (20)$$

Note that tensor S_{lk}^{ij} stays invariant with respect to interferometric baselines l, k and polarisations i, j, and is parameterized by z_o, which can be found from (20).

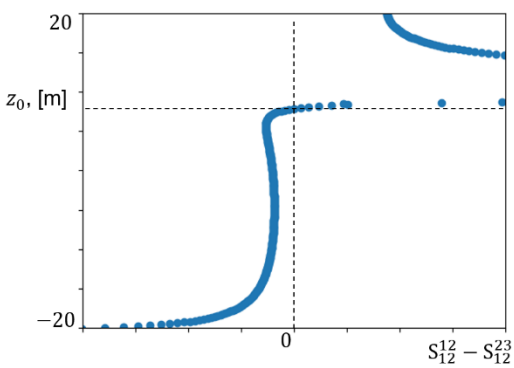

Fig. 1. Difference $S_{12}^{12} - S_{12}^{23}$ vs ground height z_0 for the two given vertical wavenumbers, $k_z^1 = 0.10$, $k_z^2 = 0.06$ and values of $\tilde{\gamma}_{Vol}^1(\vec{w})$ and $\tilde{\gamma}_{Vol}^2(\vec{w})$. Zeros of the curve, $S_{12}^{12} - S_{12}^{22} = 0$, correspond to the solutions for z_0.

Fig.1 illustrates the behavior of the curve $S_{12}^{12} - S_{12}^{23}$ with respect to the ground height z_0 for the two arbitrary vertical wavenumbers, $k_z^1 = 0.10$, $k_z^2 = 0.06$. Volumetric decorrelation values $\tilde{\gamma}_{Vol}^1(\vec{w})$ and $\tilde{\gamma}_{Vol}^2(\vec{w})$ for 3 polarisation channels were chosen arbitrary for the illustration purpose. Zeros of the curve, $L_1 - L_2 = 0$ correspond to the solutions for z_0.

Once z_0 is found, the forest height can be estimated from (16). Fig. 2 illustrates the behavior of the curve $L_1 - L_2$ with respect to the forest height h_V for the uniform ("box") vertical reflectivity profile, $F_{box} = \mathrm{rect}(\frac{z - h_V/2}{h_V})$ and the two arbitrary vertical wavenumbers, $k_z^1 = 0.10$, $k_z^2 = 0.06$. Volumetric decorrelation parameters for the illustration purpose were chosen arbitrary: $\mathrm{Im}[\tilde{\gamma}_{Vol}^1] = 0.56$, $\mathrm{Re}[\tilde{\gamma}_{Vol}^1] = 0.32$, $\mathrm{Im}[\tilde{\gamma}_{Vol}^1] = 0$, $\mathrm{Re}[\tilde{\gamma}_{Vol}^1] = -0.4$. Zeros of the curve, $L_1 - L_2 = 0$ correspond to the solutions for the forest height. The abrupt jump in $L_1 - L_2$ value occurs when forest height approaches one of the baselines ambiguity heights.

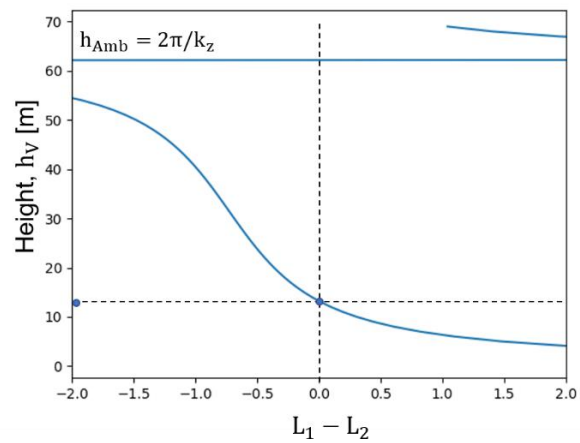

Fig. 2 Difference $L_1 - L_2$ vs height h_V for the uniform ("box") vertical reflectivity profile, two given vertical wavenumbers, $k_z^1 = 0.10$, $k_z^2 = 0.06$ and given values of: $\mathrm{Im}[\tilde{\gamma}_{Vol}^1] = 0.56$, $\mathrm{Re}[\tilde{\gamma}_{Vol}^1] = 0.32$, $\mathrm{Im}[\tilde{\gamma}_{Vol}^1] = 0$, $\mathrm{Re}[\tilde{\gamma}_{Vol}^1] = -0.4$. Zeros of the curve, $L_1 - L_2 = 0$, correspond to the solutions for the forest height.

2. DEMONSTRATION ON REAL DATA

The fully polarimetric tomographic data, used in the following, were acquired in February 2016 by DLR's F-SAR airborne sensor over the Lopé site in Gabon in the frame of the AfriSAR campaign [7] [8].

The Lopé site is located within the Lopé National Park in Gabon. The site features a variety of structure types ranging from open savannas to undisturbed tall (sometimes exceeding 50 m) dense forest stands [9] [10]. The terrain is hilly with many local slopes steeper than 20°.

As a reference, airborne Lidar data are used, collected by NASA's Land, Vegetation, and Ice Sensor (LVIS) flown onboard of a Langley B200 aircraft in February 2016 [11]. LVIS measures wide-beam full-waveforms over footprints of approximately 22m in diameter. From the measured waveforms the RH100 estimates (i.e. the height in meters from the ground where 100% of energy return occurs [12]) have been derived, interpolated and resampled to a 20 m x 20 m grid and finally transformed in UTM-coordinates. They are used as the reference forest height h_v^{ref} and are shown in Fig. 1.

100 looks fully polarimetric tomographic covariance matrices $[R_p]$ were formed, georegistered in UTM coordinates and resampled to a 20 m x 20 m grid. They were used then to estimate by SKP algorithm both ground and volume coherence matrices, $[\Gamma_{MG}]$ (taking a solution closer to the unit circle [13]) and $[\Gamma_{MV}]$ (taking a solution closer to the coherence region). The associated ground- and volume-only vertical power profiles, $P_G(z)$ and $P_V(z)$, were produced

according to (27) using a Fourier Beamforming reconstruction algorithm.

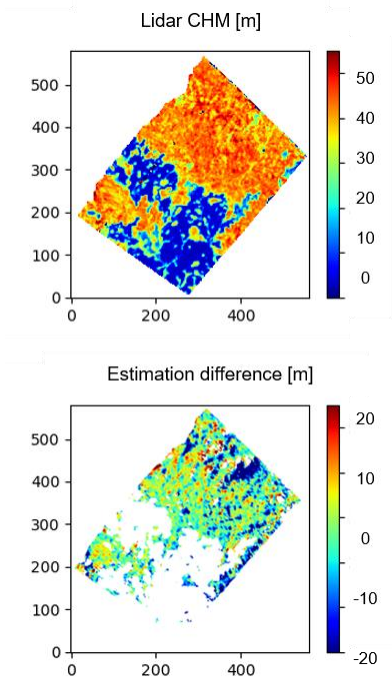

Fig. 3 Lopé test site, top: LVIS LiDAR RH100 Forest height, bottom: difference in heights estimated using dual baseline FSAR data with SKP separated volume only TomoSAR profiles and reference LVIS LiDAR RH100.

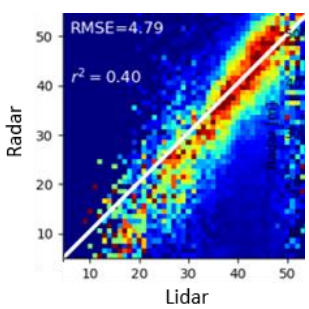

Fig. 4 Lopé forest height validation histogram relative to LiDAR RH100 reference. Dual baseline inversion performance using SKP separated volume only TomoSAR profiles

In order to use the derived vertical volume-only power profiles $P_V(z)$ in (11), they have to be cropped and normalized. The lower cropping boundary is the position of the estimated ground height. The upper boundary was estimated from the volume-only vertical power profiles from the position of 3dB attenuation of the highest peak within the interval of $z_{DEM} - 50m < z < z_{DEM} + 30m$. The cropped profiles are then resampled to the normalized unit height axis.

The dual baseline PolInSAR forest height inversion can be performed by solving the minimisation problem (13) or the equation (16). The resultant difference with the reference Lidar RH100 is illustrated by Fig. 2 while the correlation histogram is presented in Fig. 3. The dual baseline estimation allow to estimate forest with root mean square error (RMSE) of 4.79 m and correlation coefficient (r^2) of 0.40.

2. OUTLOOK

The utilization of TomoSAR-modeled profiles offers the advantage of reducing the dimensionality of the forest height inversion using complex volumetric decorrelation. This approach can aid in inverting the ground to-volume ratio and compensating for temporal decorrelation, especially advantageous for repeat-pass systems. Dual -baseline forest height inversion time can significantly be accelerated if equation (16), together with tensor invariant (20) for ground height determination, are used. These equations are invariant of temporal decorrelation and ground-to-volume ratio, reducing the intrinsically 11-parameter estimation problem into 2-parameter.

The upcoming European Space Agency BIOMASS mission, set for launch in 2025, will gather tomographic, polarimetric, and interferometric data [16]. The algorithm proposed by this paper is applicable to this mission, capitalizing on the entire spectrum of collected data.

The developed algorithm has primarily been tested in tropical forests, but have the potential for global applicability. The careful consideration of baseline variations is important, as the spaceborne missions acquire interferometric data with varying baseline setups.

4. REFERENCES

[1] R. Treuhaft and P. Siqueira, "Vertical structure of vegetated land surfaces from interferometric and polarimetric radar," *Radio Science,* vol. 35, no. 1, pp. .141-177, 2000.

[2] S. Cloude, Polarisation: applications in remote sensing, Oxford: OUP , 2009.

[3] A. Reigber and A. Moreira, " First demonstration of air-borne SAR tomography using multibaseline L-band data," *IEEE Trans. Geosci. Remote Sens.,* vol. 38, no. 5, pp. 2142-2152, Sept. 2000.

[4] S. Tebaldini, "Algebraic synthesis of forest scenarios from multibaseline PolInSAR data," *IEEE Trans. Geosci. Remote Sens.,* vol. 47, no. 12, p. 4132–4142, 2009.

[5] F. Lombardini and A. Reigber, "Adaptive spectral estimation for multibaseline SAR tomography with airborne L-band data," in *IGARSS IEEE International*

Geoscience and Remote Sensing Symposium IEEE Proceedings (IEEE Cat. No. 03CH37477), 2003.

[6] S. Lee, F. Kugler, K. Papathanassiou and I. Hajnsek, "Quantification of temporal decorrelation effects at L-band for polarimetric SAR interferometry applications," *IEEE Journal of Selected Topics in Applied Earth Observations and Remote Sensing*, 2013.

[7] I. Hajnsek, M. Pardini, et al.,, "Technical assistance for the development of airborne SAR and geophysical measurements during the AfriSAR campaign, Final technical report".

[8] T. Fatoyinbo et al., "The NASA AfriSAR campaign: Airborne SAR and lidar measurements of tropical forest structure and biomass in support of current and future space missions," vol. 264, p. 112533, 2021.

[9] N. Labriere et al, "In Situ Reference Datasets from the TropiSAR and AfriSAR Campaigns in Support of Upcoming Spaceborne Biomass Missions," *IEEE J. Sel. Top. Appl. Earth Obs. Remote Sens*, vol. 11, no. 10, p. 3617–3627, 2018.

[10] S. M. Marselis, H. Tang, J. D. Armston, K. Calders, N. Labrière and R. Dubayah, "Distinguishing vegetation types with airborne waveform lidar data in a tropical forest-savanna mosaic: A case study in Lopé National Park, Gabon," *Remote Sens. Environ*, vol. 216, no. 626–634, 2018.

[11] J. Blair and M. Hofton, "AfriSAR LVIS L2 Geolocated Surface Elevation Product, Version 1. Boulder, Colorado USA. NASA National Snow and Ice Data Center Distributed Active Archive Center," [Online]. [Accessed 2018].

[12] R. O. Dubayah et al., "Estimation of tropical forest height and biomass dynamics using lidar remote sensing at La Selva, Costa Rica," *," J. Geophys Res.,* vol. 115, 2010.

[13] S. Tebaldini and F. Rocca, "Multibaseline polarimetric SAR tomography of a boreal forest at P- and L-bands," *IEEE Transactions on Geoscience and Remote Sensing*, vol. 50, no. 1, pp. 232-246, 2011.

[14] M. Pardini, M. Tello, V. Cazcarra-Bes, K. Papathanassiou and I. Hajnsek, "L-and P-band 3-D SAR reflectivity profiles versus lidar waveforms: The AfriSAR case.," *IEEE Journal of Selected Topics in Applied Earth Observations and Remote Sensing*, vol. 1, 2018.

[15] M. Pardini, V. Cazcarra-Bes and K. P. Papathanassiou, "TomoSAR Mapping of 3D Forest Structure: Contributions of L-Band Configurations," *Remote Sensing*, vol. 13, no. 12, p. 2255, 2021.

[16] S. Quegan, T. Le Toan, J. Chave, J. Dall, J. Exbrayat, D. Minh, M. Lomas, M. D'alessandro, P. Paillou, K. Papathanassiou and F. Rocca, "The European Space Agency BIOMASS mission: Measuring forest above-ground biomass from space," *Remote Sensing of Environment*, no. 227 , pp. 44-60, 2019.